Electronic structure of cleaved-edge-overgrowth strain-induced quantum wires

M. Grundmann, O. Stier, A. Schliwa, and D. Bimberg
Institut für Festkörperphysik, Technische Universität Berlin, Hardenbergstrasse 36, D-10623 Berlin, Germany
(Received 8 June 1999; revised manuscript received 21 July 1999)

The electronic properties of strained cleaved-edge-overgrowth quantum wires are calculated for structures in which the (001) quantum well has a larger lattice constant and band gap than the barrier and imposes tensile strain on the (110) quantum well. The lateral charge-carrier confinement is entirely due to strain effects and not due to heterostructure barriers. Large localization energies of up to 90 meV are predicted from eight band $\mathbf{k}\cdot\mathbf{p}$ calculations. Symmetric, asymmetric, and interdiffused geometries in the $In_{0.2}Al_{0.8}As/Al_{0.35}Ga_{0.65}As/GaAs$ system are investigated.

Cleaved-edge overgrowth (CEO) has been used in recent years to fabricate quantum wires (QWR) (Refs. 1 and 2) and quantum dots.[3–5] The inclusion of *strained* layers in such structures introduces a new dimension in band-gap engineering and may strongly modify confinement effects. Theoretical investigations of the electronic states for structures consisting of lattice matched materials have been presented by several groups.[3,6–9] The confinement in this case is a consequence of the configuration of the heterostructure barriers. In Ref. 10, the effects of compressively strained material for both the (001) and (110) layers in the conventional T-shape geometry have been theoretically analyzed. No distinctive enhancement of carrier confinement at the juncture due to strain effects was identified.

In this work we study the configuration proposed in Ref. 11 and sketched in Fig. 1. The (001) layer ($In_{0.2}Al_{0.8}As/Al_{0.35}Ga_{0.65}As$) is compressively strained by the GaAs substrate and exerts tensile strain on the (110) quantum well (QWL) and barrier, in our case $GaAs/Al_{0.35}Ga_{0.65}As$. The band gap of the (001) $In_{0.2}Al_{0.8}As$ layer is sufficiently high that the charge carriers are confined to the (110) GaAs layer. This configuration of the CEO structure creates a new physical situation: The lateral charge-carrier localization (along [110]) is not due to heterostructure barriers but solely due to the induced tensile strain in the (110) layer.

First the strain for the given structure is calculated by minimizing the strain energy. Here we use the continuum mechanical (CM) model.[10,14] The material parameters used in the calculations are shown in Table I. The extension of the strained region used for the CM calculations in the [110] direction is large (about 180 nm) and only a fraction close to the QWR is shown in all graphs. In the [001] direction, periodic boundary conditions (i.e., a superlattice) are assumed. A comparison with a single QWR will also be made. In Fig. 2, three strain components (ε_{xx}, ε_{zz}, and ε_{xy}) and the hydrostatic strain $\varepsilon_H=\varepsilon_{xx}+\varepsilon_{yy}+\varepsilon_{zz}$ around the juncture are shown. The results from CM strain relaxation will be compared with the ''pseudomorphic strain'' (PS) model in which two subsequent pseudomorphic growth steps are assumed, first in the (001) direction and then in the (110) direction. The PS model yields several regions of constant strain without allowing for proper strain relaxation.

The band-structure calculation is carried out within eight-band $\mathbf{k}\cdot\mathbf{p}$ theory, used by us previously for V-groove quantum wires.[15] The model accounts for valence-band mixing and conduction-band–valence-band interaction. The $\mathbf{k}\cdot\mathbf{p}$ Hamiltonian is solved on $40\times40\,nm^2$ areas. First we calculate electron and hole levels for a *symmetric* geometry where both layers have the same width ($d_{100}=d_{110}=10$ nm), for the two cases of a (001) superlattice (30-nm $Al_{0.35}Ga_{0.65}As$ barriers) and a single QWR. Additionally, *asymmetric* wires and the effect of intermixing [indium diffusion from the $In_xAl_{1-x}As$ layer into the (110) GaAs quantum well] are investigated.

Significant differences between the CM and PS strain models are found. In particular, the hydrostatic strain, responsible for the shift of the conduction band, differs near the junction by about 0.012. In Fig. 3, line scans of ε_{zz} and of the hydrostatic strain are shown along the [110] direction.

Using eight-band $\mathbf{k}\cdot\mathbf{p}$ theory we find the levels given in Table II. Also given is the optical recombination energy (without Coulomb effects). The wave functions in the QWR are shown in Fig. 4. As expected, the wave functions are entirely confined to the (110) GaAs QWL and do not penetrate into the $In_xAl_{1-x}As$ layer.

Due to the different strain distributions, the positions of the electron and hole levels differ between the cases of a superlattice and a single QWR. However, the optical recombination energy is very similar. With respect to the quantum-well energy levels, which act as barriers for the localized QWR states, both the electrons and holes are predicted to have about 30 meV localization energy. The numerical results are shown in Table III, together with the values for

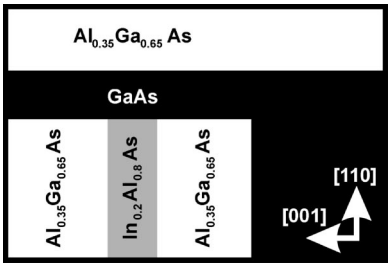

FIG. 1. Geometry of strained CEO quantum wire. Numerical examples are calculated for the $In_{0.2}Al_{0.8}As/Al_{0.35}Ga_{0.65}As/GaAs$ system.

 ©2000 The American Physical Society

TABLE I. Low-temperature material parameters of GaAs, $Al_{0.35}Ga_{0.65}As$, and $In_{0.2}Al_{0.8}As$ used in the calculations (from Refs. 12 and 13): Lattice constant a_0, band gap E_g, average valence-band position $E_{v,\mathrm{av}}$, spin-orbit splitting Δ_0, elastic constants C_{11}, C_{12}, and C_{44}, hydrostatic deformation potentials for the band gap a and the conduction band a_c, shear deformation potentials b ([110]) and d ([111]), electron mass m_e, Luttinger parameters γ_1, γ_2, and γ_3, the static dielectric constant ε_s, and the piezoelectric module e_{14}.

	GaAs	$Al_{0.35}Ga_{0.65}As$	$In_{0.2}Al_{0.8}As$
a_0 (nm)	0.565 33	0.565 596	0.574 054
E_g (eV)	1.519	2.022 4	2.563 2
$E_{v,\mathrm{av}}$ (eV)	−6.92	−7.12	−7.326
Δ_0 (eV)	0.34	0.327	0.314
C_{11} (10^{10} Pa)	11.81	11.88	11.28
C_{12} (10^{10} Pa)	5.38	5.49	5.47
C_{44} (10^{10} Pa)	5.94	5.92	5.50
a (eV)	−9.77	−8.556	−6.24
a_c (eV)	−7.1	−5.91	−4.04
b (eV)	−1.8	-1.70	1.56
d (eV)	−3.6	−3.53	−3.44
m_e	0.066 5	0.095 7	0.125
γ_1	6.79	5.62	6.69
γ_2	1.92	1.49	2.27
γ_3	2.78	2.26	2.89
ε_s	13.18	12.38	11.64
e_{14} (cm^{-2})	0.16	0.183	0.189

other geometries discussed below. Excited hole levels (with one and two nodes along [001], respectively) are found at 7 and 13 meV above the hole ground state. The ground-state recombination energy of the QWR is expected well below

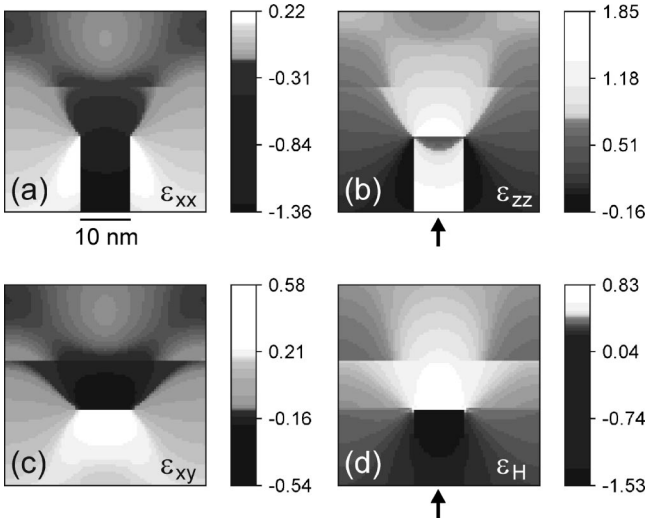

FIG. 2. Strain components (a) ε_{xx}, (b) ε_{zz}, (c) ε_{xy}, and (d) $\varepsilon_H=\varepsilon_{xx}+\varepsilon_{yy}+\varepsilon_{zz}$ for the geometry shown in Fig. 1, assuming periodic boundary conditions [i.e., a (001) superlattice] at the right and left sides of the depicted region ($40\times40\ \mathrm{nm}^2$). The x, y, and z directions are [100], [010], and [001], respectively. Nonlinear gray scales have been used to highlight the variation of strain around the juncture. The arrows denote the position of the line scans shown in Fig. 3.

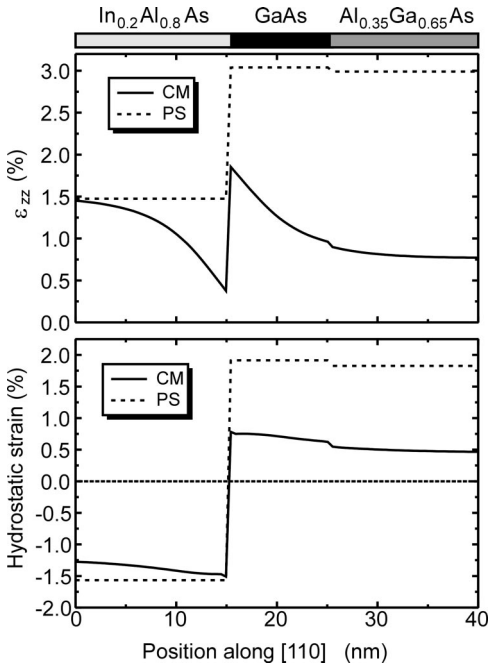

FIG. 3. Line scans of the ε_{zz} strain component and the hydrostatic strain ε_H along [110] through the center of the $In_xAl_{1-x}As$ quantum well for the continuum mechanical (CM) and pseudomorphic strain (PS) models. The position of the line scans is visualized in Fig. 2 by arrows.

(≈60 meV) the QWL recombination. An enhanced exciton binding energy of the QWR exciton with respect to the QWL exciton will increase this value in the order of 10 meV. The PS model largely overestimates the localization effects by a factor of 3 (≈190 meV).

For a structure with smaller (110) QWL thickness, $d_{110}=5$ nm, both electron and hole levels are more strongly confined along [110] and shifted in energy. The localization energies with respect to the QWL levels remain similar. The recombination energies of QWR and QWL are blueshifted as compared to the $d_{110}=10$ nm structure, but their difference remains similar (about 55 meV).

An increase of localization energy is predicted for a structure with increased thickness of the (001) QWL. For $d_{001}=15$ nm, which for the given mismatch should still be below the critical thickness for dislocation formation,[16] and d_{110}

TABLE II. Electron (E_e) and hole (E_h) energy levels as well as optical recombination energy ($E_{e\text{-}h}$) for strained CEO QWR's and (110) $GaAs/Al_xGa_{1-x}As$ QWL. For all structures $d_{001,\mathrm{In}_x\mathrm{Al}_{1-x}\mathrm{As}}=10$ nm and $d_{110,\mathrm{GaAs}}=10$ nm. For the CM model a superlattice (SL) ($d_{001,\mathrm{Al}_x\mathrm{Ga}_{1-x}\mathrm{As}}=30$ nm) and a single QWR are compared. The CM and PS strain models are compared for the SL case. Also the values for a $GaAs/Al_xGa_{1-x}As$ quantum well are given. The unstrained GaAs conduction-band edge is chosen as the origin of the energy axis.

Geometry	Strain model	E_e (meV)	E_h (meV)	$E_{e\text{-}h}$ (meV)
SL-QWR	CM	−1.8	−1501.3	1497.5
Single QWR	CM	17.6	−1514.5	1496.9
SL-QWR	PS	−67.8	−1435.5	1367.7
QWL	CM	32.6	−1527.4	1560.0

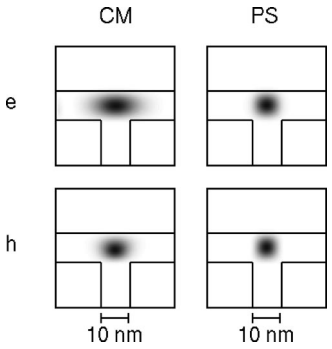

FIG. 4. Wave functions for the lowest electron and hole levels in 10 nm/10 nm $In_{0.2}Al_{0.8}As/Al_{0.35}Ga_{0.65}As/GaAs$ QWR (superlattice) for CM and PS strain models.

$=10$ nm, a total localization energy of 87 meV is predicted. In this case, the first excited electron (hole) level is separated by 14.9 (7.3) meV, yielding an excited-state transition separated about 22 meV from the ground state.

Finally, we have investigated the effect of indium diffusion from the $In_xAl_{1-x}As$ into the GaAs QWL [and the surrounding $Al_xGa_{1-x}As$ (Ref. 17)]. For an indium diffusion length of $L_D=5$ nm, we did not find any significant changes (see Table III) because the effect of a locally decreased $In_xGa_{1-x}As$ band gap at the $In_xAl_{1-x}As/GaAs$ junction is offset by the simultaneous modification of the strain distribution.

The calculated localization energies are a lower limit because up to this point the piezoelectric effect has not been included. Shear strains lead to the formation of piezoelectric charges and give rise to an additional potential.[14,18] In the present case, the potential in the (110) QWL has dipole character along (001) and tends to separate electrons and holes away from the center of the (001) QWL. In the 10 nm/10 nm structure, electrons (holes) show a shift of 10 (11.8) meV due to piezoelectricity, such that the localization energy increases (and the recombination energy decreases) by an additional 22 meV.

In summary, we have theoretically investigated strain-induced CEO quantum wires. We have used the continuum mechanical model for the strain calculation and eight-band $\mathbf{k}\cdot\mathbf{p}$ theory for the calculation of the electronic states. The pseudomorphic strain approximation has been found to be completely inappropriate. As an example, the $In_{0.2}Al_{0.8}As/Al_{0.35}Ga_{0.65}As/GaAs$ system has been modeled. For typical QWL thicknesses of 5–10 nm, sizable localization energies for electrons and holes of about 30 meV each are predicted. An indium diffusion out of the stressor QWL is not found to lead to significant modifications of the electronic states.

TABLE III. Electron (E_e) and hole (E_h) energy levels as well as optical recombination energy ($E_{e\text{-}h}$) for strained CEO QWR and (110) $GaAs/Al_xGa_{1-x}As$ QWL. The layer thicknesses of the (001) and (110) QWL's vary as indicated. $L_D=5$ nm denotes the indium diffusion length. All numbers are based on the CM strain model. The unstrained GaAs conduction-band edge is chosen as the origin of the energy axis.

Geometry	d_{001} (nm)	d_{110} (nm)	E_e (meV)	E_h (meV)	$E_{e\text{-}h}$ (meV)
SL-QWR	10	10	−1.8	−1501.3	1497.5
SL-QWR $L_D=5$ nm	10	10	−2.8	−1502.0	1499.2
SL-QWR	15	10	−16.3	−1489.7	1473.4
SL-QWR	10	5	50.3	−1524.7	1575.0
QWL		10	32.6	−1527.4	1560.0
QWL		5	78.7	−1541.0	1619.7

The predicted localization energy of about 90 meV for an asymmetric QWR surpasses the largest values reported so far for T-shape QWR's, 38 meV for an asymmetric GaAs/AlAs structure,[19] 34 meV for a 3.5-nm $In_{0.17}Ga_{0.83}As/Al_{0.3}Ga_{0.7}As$ structure,[20] and 54 meV for an optimized asymmetric QWR consisting of a $GaAs/Al_{0.3}Ga_{0.7}As$ layer on $Al_{0.12}Ga_{0.88}As/Al_{0.3}Ga_{0.7}As$.[21] We conclude that CEO QWR's with the (001) QWL laid out as a stressor are an interesting one-dimensional system to achieve improved temperature stability.

We are grateful to D. Gershoni for stimulating discussions. This work was supported by Deutsche Forschungsgemeinschaft in the framework of Sfb 296.

[1] L. Pfeiffer, K. W. West, H. L. Störmer, J. P. Eisenstein, K. W. Baldwin, D. Gershoni, and J. Spector, Appl. Phys. Lett. **56**, 1697 (1990).

[2] T. Someya, H. Akiyama, and H. Sakaki, Phys. Rev. Lett. **74**, 3664 (1995).

[3] M. Grundmann and D. Bimberg, Phys. Rev. B **55**, 4054 (1997).

[4] D. Bimberg, M. Grundmann, and N. N. Ledentsov, *Quantum Dot Heterostructures* (Wiley, Chichester, 1998).

[5] W. Wegscheider, G. Schedelbeck, G. Abstreiter, M. Rother, and M. Bichler, Phys. Rev. Lett. **79**, 1917 (1997).

[6] A. A. Kiselev and U. Rössler, Semicond. Sci. Technol. **11**, 203 (1996).

[7] L. Pfeiffer, H. Baranger, D. Gershoni, K. Smith, and W. Wegscheider, in *Low Dimensional Structures Prepared by Epitaxial Growth or Regrowth on Patterned Substrates*, edited by K. Eberl, P. M. Petroff, and P. Demeester (Kluwer Academic, Dordrecht, 1995), p. 93.

[8] W. Langbein, H. Gislason, and J. M. Hvam, Phys. Rev. B **54**, 14 595 (1996).

[9] S. Glutsch, F. Bechstedt, W. Wegscheider, and G. Schedelbeck, Phys. Rev. B **56**, 4108 (1997).

[10] M. Grundmann, O. Stier, and D. Bimberg, Phys. Rev. B **58**, 10 557 (1998).

[11] D. V. Regelman and D. Gershoni, *Proceedings of the 24th International Conference on the Physics of Semiconductors*, edited by D. Gershoni (World Scientific, Singapore, 1999), p. 1111.

[12] D. Gershoni, C. H. Henry, and G. A. Baraff, IEEE J. Quantum Electron. **QE-29**, 2433 (1993).

[13] *Physics of Group IV Elements and III-V Compounds*, edited by O. Madelung, M. Schulz, and H. Weiss, Landolt-Börnstein Numeri-

cal Data and Relationships, New Series, Group III, Vol. 17a (Springer, Berlin, 1982).
[14] O. Stier, M. Grundmann, and D. Bimberg, Phys. Rev. B **59**, 5688 (1999).
[15] O. Stier and D. Bimberg, Phys. Rev. B **55**, 7726 (1997).
[16] M. Grundmann, U. Lienert, J. Christen, D. Bimberg, A. Fischer-Colbrie, and J. N. Miller, J. Vac. Sci. Technol. B **8**, 751 (1990).
[17] Strictly speaking, we assume Fickian interdiffusion of In and Ga, while the Al distribution remains fixed.
[18] M. Grundmann, O. Stier, and D. Bimberg, Phys. Rev. B **50**, 14 187 (1994).
[19] T. Someya, H. Akiyama, and H. Sakaki, Phys. Rev. Lett. **76**, 2965 (1996).
[20] H. Akiyama, T. Someya, M. Yoshita, T. Sasaki, and H. Sakaki, Phys. Rev. B **57**, 3765 (1998).
[21] W. Langbein, H. Gislason, and J. M. Hvam, Phys. Rev. B **54**, 14 595 (1996); H. Gislason, W. Langbein, and J. M. Hvam, Appl. Phys. Lett. **69**, 3248 (1996).